Journal of Nuclear Materials 403 (2010) 121–125

Contents lists available at ScienceDirect

Journal of Nuclear Materials

journal homepage: www.elsevier.com/locate/jnucmat

Peculiarities of plastic flow involving "deformation waves" observed during low-temperature tensile tests of highly irradiated 12Cr18Ni10Ti and 08Cr16Ni11Mo3 steels

M.N. Gusev [a,*], O.P. Maksimkin [a], F.A. Garner [b]

[a] Institute of Nuclear Physics, Ibragimov str., 1, Almaty 050032, Kazakhstan
[b] Radiation Effects Consulting, Richland, WA 99354, USA

ARTICLE INFO

Article history:
Received 29 October 2009
Accepted 7 June 2010

ABSTRACT

In a previous paper, it was shown that the expectation that neutron irradiation of low-nickel austenitic steels leads to a low saturation level of ductility is not always valid. At high dose ductility is observed first to decrease with dpa during room temperature testing and then under some conditions to increase at higher dose. This produces anomalously high deformation arising from a previously unrecognized mechanism that precludes sustained necking and produces a moving deformation front. It was earlier speculated that this behavior is a result of α-martensite formation in the deforming region. New studies involving testing over −115 to +120 °C confirm that the $\gamma \rightarrow \alpha$ transformation is involved with this deformation mechanism and is the cause of the recaptured ductility. When the irradiated alloy has not yet reached the dose threshold of wave initiation at room temperature a decrease in test temperature can induce wave generation, consistent with the known effect of temperature on martensite instability.

1. Introduction

In our previous paper [1], we demonstrated that under some conditions the well-known trend toward reduction and saturation of elongation with increasing exposure at low irradiation temperature is reversed at higher neutron dose (26–55 dpa). We showed that improved or recaptured levels of ductility occur via a previously unanticipated change in deformation mechanism involving a radiation-induced wave front of deformation that proceeds along the length of the specimen in response to an inability of the specimen to sustainably form a neck. We speculated that a martensitic instability was occurring in the deformed region, hardening the material such that deformation was shifted away from the nascent neck into the undeformed material ahead of the wave front.

In this paper we present the results of new studies that confirm the involvement of the $\gamma \rightarrow \alpha$ transformation to produce the deformation wave, and that explore the influence of alloy composition, displacement dose and test temperature in the range −115 to +120 °C.

2. Experimental details

Hexagonal wrappers constructed from 12Cr18Ni10Ti and 08Cr16Ni11Mo3 steels (Russian analogs of AISI 321 and 316) with nominal composition in wt.%: 0.10–0.12%C, 17.5–19%Cr, 9–10.5%Ni, 0.5%Ti and 0.08C, 11.5Ni, 16Cr, 3Mo, respectively) were removed from a number of spent fuel assemblies after irradiation in the BN-350 fast reactor. The wrappers had a face-to-face distance of 96 mm and walls that were 2 mm thick. Prior to irradiation the wrappers were formed with cold deformation of 15–20%, followed by annealing at 800°C for an hour. The irradiation conditions of the specimens chosen for testing are shown in Table 1.

Cross sections of 10 mm height were cut from the wrappers at various elevations between +500 mm and −160 mm, measured relative to the core center-plane. From these sections flat rectangular specimens were mechanically produced with dimensions 20 mm in length, 2 mm in width and 0.3 mm in thickness. Subsequently, mini-tensile specimens with gauge length of 7–10 mm, width of 2 mm and thickness of 0.3 mm were produced by mechanical grinding and electrolytic polishing to achieve the desired dimensions and surface quality.

Pneumatic grips were used for holding the specimen in an Instron-1195 tensile machine. Uniaxial tensile tests on both unirradiated and irradiated specimens were performed at strain rate of $8.3 \times 10^{-4}\ \mathrm{sec}^{-1}$. Limited numbers of specimens were also tested at $8.3 \times 10^{-3}\ \mathrm{sec}^{-1}$ and $8.3 \times 10^{-5}\ \mathrm{sec}^{-1}$. The specimens were tested in the range from −115 to +120°C. The temperatures were maintained at high temperatures by electrical heating. Testing at cryogenic temperatures was performed using an Instron A 74–1100 temperature cabinet modified for the use of liquid nitrogen. The precision and stability of temperature during the test was ±5 °C.

* Corresponding author. Tel.: +7 727 386 68 00x371; fax: +7 727 386 52 60.
E-mail address: gusev.maxim@inp.kz (M.N. Gusev).

0022-3115/$ - see front matter © 2010 Elsevier B.V. All rights reserved.
doi:10.1016/j.jnucmat.2010.06.010

Table 1
Position and irradiation conditions of investigated samples of 12Cr18Ni10Ti and 08Cr16Ni11Mo3.

Steel	Assembly code	Distance from the center of the core (mm)	Irradiation temperature (°C)	Dose (dpa)
12Cr18Ni10Ti	H-42	−300	290	13
12Cr18Ni10Ti	CC-19	+500	423	26
12Cr18Ni10Ti	CC-19	−160	310	55
12Cr18Ni10Ti	H-214-1	0	337	17
08Cr16Ni11Mo3	B-300	−500	302	11
08Cr16Ni11Mo3	B-337	−500	305	12
08Cr16Ni11Mo3	H-214(2)	−900	281	1.27

During tensile experiments a technique called "digital marker extensometry" [2,3] was used. With this technique it is possible to obtain the true stress–true strain behavior for a miniature specimen, as well as to identify the localized deformation region and to trace its evolving geometry during continuous deformation.

Video-recording was applied at all test temperatures, but for cryogenic temperatures the resolution of the record is reduced because of the longer specimen to camera distance. Therefore the record at cryogenic temperatures is used primarily to establish whether a moving deformation wave occurs or not. A combination of magnetometry, metallography and microhardness measurements was used to determine the existence, level and distribution of α-martensite.

The measurement of the amount of martensite was performed with a Fisher-MP-30 ferroprobe. For translation from dimensionless "ferrite numbers" to volumetric martensite amount a set of probes with known amount of martensite were used as standards. The etalon probe set was produced by using X-radiography and density measurements according to Ref. [4]. Some etalons were fabricated from pure iron powder as described in Ref. [5]. Aspects of etalon probe fabrication and scale factors for sample thickness corrections are described in detail in Ref. [6].

3. Experimental results

It was confirmed that when a moving wave form of deformation was observed it was accompanied by a $\gamma \rightarrow \alpha$ martensitic transformation has indeed occurred in the deformed area immediately behind the wave front. While the amount of martensite in a deformed unirradiated specimen averages about 5–10% in volume [4,7] the volume of martensite behind the wave is 30–35% in a specimen irradiated to 26 dpa at 423 °C, as shown in Fig. 1. The stress–strain curve for this specimen is designated as #4 in Fig. 2.

The measured values of strength and ductility at room temperature are shown in Table 2 for different test temperatures and applied strain rates. In Fig. 2, it can be seen that the unirradiated steel is characterized by high ductility and a high ability to strain-harden with the ultimate stress σ_B significantly greater than the yield stress σ_{02}. As the dose increases one can see that irradiation of 12Cr18Ni10Ti and 08Cr16Ni11M03 to doses of <20 dpa leads to substantial increases in yield stress and reduction of ductility, a behavior consistent with that of many previous studies [8–11]. A neck develops very quickly after the yield point, quickly leading to localized failure while most of the specimen does not participate in the deformation. At higher doses however, the anomalous behavior asserts itself. Note that after a small decrease in strength following yielding there is an extended plateau without significant increase in load.

In the 26 or 55 dpa cases where anomalous ductility was observed a stable immobile neck did not develop. The boundary of the localized deformation band moves, producing a moving deformation front that travels along the length of the specimen. In the 55 dpa specimen tested at 20 °C the wave front moved at ~0.04 mm/s while the applied strain rate to the specimen was only 0.008 mm/s, reflecting a concentration of the deformation at the wave front. The local deformation behind the wave front is usually in the 30–40% range.

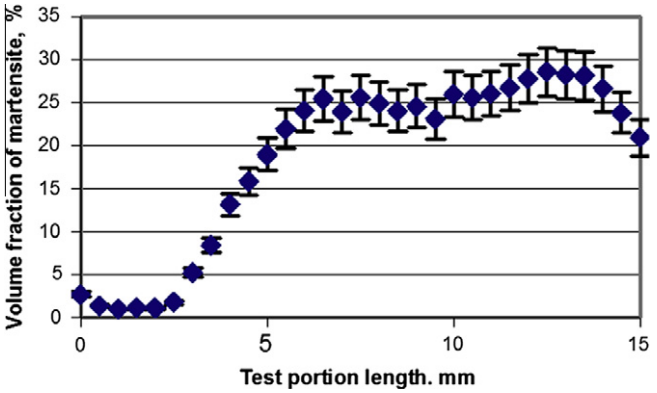

Fig. 1. Distribution of α′-martensite amount along the specimen length (12Cr18Ni10Ti, 26 dpa, deformed at 20 °C). The deformation was interrupted when the wave had reached the 4–5 mm position. Direction of wave movement is from right to the left.

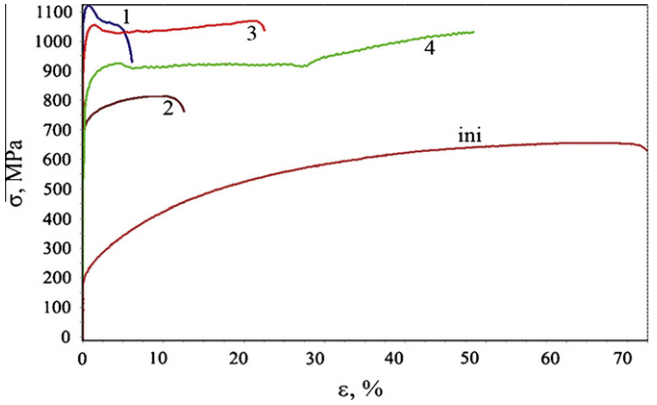

Fig. 2. Engineering stress–strain curves for an unirradiated (ini) specimen of 12Cr18Ni10Ti and irradiated specimens; curve #1, 08Cr16Ni11Mo3, 11 dpa; #2, 08Cr16Ni11Mo3, 1.27 dpa; #3, 12Cr18Ni10Ti, dose 55 dpa; #4, 12Cr18Ni10Ti, 26 dpa. All tests were conducted at 20 °C.

Sometimes these waves started near each grip and progressed in opposite directions. Usually the second wave begins just after the first wave stops. There was one example, however, where simultaneous movement of two waves was observed. When two waves occurred, this produced the highest total engineering deformation of 40–48%.

In most cases the wave front is defined by a simple straight line at an angle of 45–50° to the deformation axis, but sometimes the wave front exhibits a corner (intersection of two straight lines) that is probably the result of two initiation sites occurring on opposite sides of the specimen at nearly the same axial location (see Fig. 3a).

Specimens of 12Cr18Ni10Ti irradiated to 26 dpa were tested in the interval 8.3×10^{-3} to $8.3 \times 10^{-5}\ s^{-1}$. Since the martensitic transformation is known to be sensitive to the speed of deformation one might expect the test speed to influence the occurrence of deformation waves, primarily due to temperature rises associated with martensite formation and heat retention in larger specimens. However, as shown in Table 2, a variation of deformation speed by one order of magnitude did not lead to disappearance

Table 2
Mechanical properties of investigated samples.

Steel, assembly, level (mm)	Dose (dpa)	Test temperature (°C)	Strain rate (s^{-1})	σ_{02} (MPa)	σ_B (MPa)	ε_u (%)	ε_T (%)	Presence of wave
12Cr18Ni10Ti, unirradiated steel	–	20	8.3×10^{-4}	200	650	65	73	No
12Cr18Ni10Ti, H-42, −300	13	20	8.3×10^{-4}	860	1010	3	7	No
12Cr18Ni10Ti, H-42, −300	13	−40	8.3×10^{-4}	1030	1110	~1	53	Yes[a]
12Cr18Ni10Ti, CC-19, +500	26	20	8.3×10^{-4}	780	930	18	18.5	Yes
12Cr18Ni10Ti, CC-19,+500	26	20	8.3×10^{-3}	800	1030	48	48	Yes[a]
12Cr18Ni10Ti, CC-19, +500	26	20	8.3×10^{-5}	790	950	21	21.5	Yes
12Cr18Ni10Ti, H-214-1, 0	17	20	8.3×10^{-4}	980	1120	<2	5	No
12Cr18Ni10Ti, H-214-1, 0	17	−50	8.3×10^{-4}	980	1120	2.0	23	Yes
12Cr18Ni10Ti, CC-19, −160	55	20	8.3×10^{-4}	960	1070	20	22	Yes
12Cr18Ni10Ti, CC-19, +500	26	60	8.3×10^{-4}	740	850	40	43	Yes[a]
12Cr18Ni10Ti, CC-19, −160	55	120	8.3×10^{-4}	940	980	~1	<4	No
08Cr16Ni11Mo3, H-214-2, −900	1.27	20	8.3×10^{-4}	710	820	11	13	No
08Cr16Ni11Mo3, B-300, −500	11	20	8.3×10^{-4}	970	1100	1.5	4	No
08Cr16Ni11Mo3, B-300, −500	11	−40	8.3×10^{-4}	1200	1270	1.5	12	No
08Cr16Ni11Mo3, B-300, −500	11	−80	8.3×10^{-4}	1110	1270	1	7	No
08Cr16Ni11Mo3, B-300, −500	12	−115	8.3×10^{-4}	1130	1370	27	28	Yes[a]

σ_{02}, σ_B, ε_u, ε_T are the yield and ultimate stresses, uniform and total elongation, respectively.
[a] Samples having two deformation waves are marked with a star.

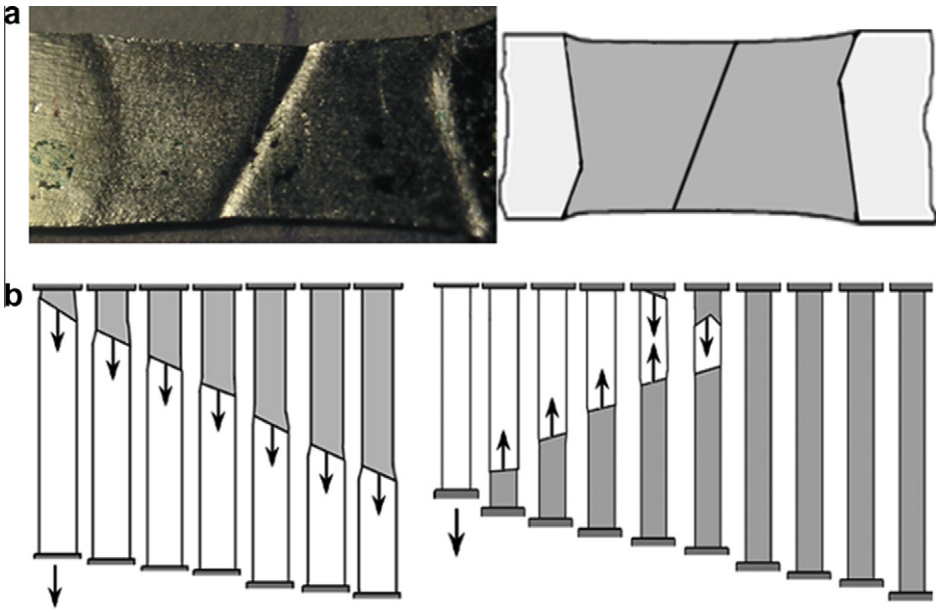

Fig. 3. Image and schematic representation of various complex deformation wave fronts. (a) One can see two deformation zones, each developing behind a moving wave front originating from an attempted neck. Deformation of this specimen was stopped before failure occurred. (b) Schematic illustrations of deformation waves for single-wave (left) and double-wave (right) cases. A typical single-wave starts moving from one grip and stops at about 2/3 of sample length. Shortly after the first wave stops the second wave starts from the other grip. In the two-wave case there is usually no undeformed space remaining on the specimen at failure.

of deformation waves, probably because the small specimen size did not favor significant heat retention over this range of deformation rates.

Whereas testing at room temperature and above leads to sustained necking and reduced ductility, a decrease in the test temperature to −40 or −50 °C induces wave formation and increases the plasticity of 12Cr18Ni10Ti steel to 20–50%, as seen in Table 2 and Fig. 4. To generate a wave in the 08Cr18Ni11Mo3 steel one needs to use a temperature of −115 °C and below. This behavior is expected because this higher-nickel, higher molybdenum steel is known to be more stable against martensite formation compared to 12Cr18Ni10Ti.

One can see from Table 3 that decreasing the deformation temperature leads to an increase in martensite. It appears that the formation of a deformation wave can take place if the amount of martensite exceeds 25–30%. While levels of martensite in unirradiated 12Cr18Ni10Ti usually reached only 5–10% after deformation to failure, levels of 30–35% were observed after deformation of specimens that experienced high displacement doses.

One uninvestigated question concerns the kinetics of martensite formation during wave formation in irradiated steels. If it is too rapid there may not be much plasticity and if too slow a wave may not develop.

4. Discussion

Fig. 5 presents stress–deformation curves for both 26 and 55 dpa specimens tested at room temperature using the digital extensometry technique. Almost immediately on reaching the

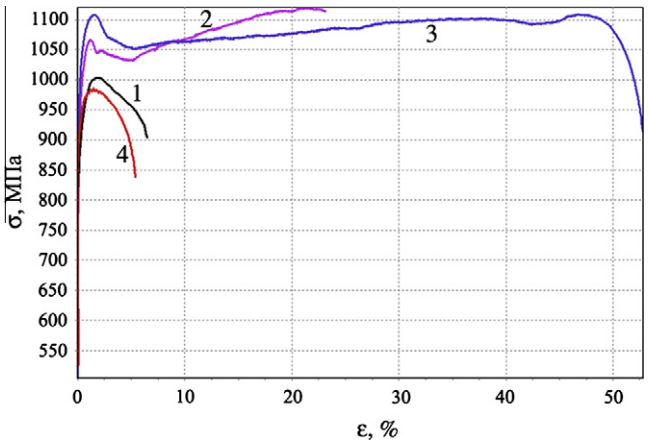

Fig. 4. Engineering curves for 12Cr18Ni10Ti. Curve #1, 13 dpa, tested at 20 °C; #2, 17 dpa, tested at −50 °C; #3, 13 dpa, tested at −40 °C; #4, 55 dpa, tested at 120 °C, showing that low temperature deformation can induce wave formation at dpa levels insufficient to generate waves at room temperature or above.

Table 3
Amount of α-martensite measured in highly-irradiated samples of investigated steels after deformation.

Assembly, level, dose, steel	Deformation temperature (°C)	Amount of martensite, relative unit	Amount of martensite (vol.%)	Estimated local deformation at point of measurement
CC-19, −160 55 dpa 12Cr18Ni10Ti	20 120	7.5 <0.1	35 <0.2	0.3–0.35 0.5–0.7
H-42, −300 13 dpa 12Cr18Ni10Ti	20 −40	0.85 10.8	4 40	– 0.35–0.4
B-337, −500 12 dpa 08Cr16Ni11Mo3	20 −115	2.2 10.2	8–9 37	0.5–0.6 0.4–0.45

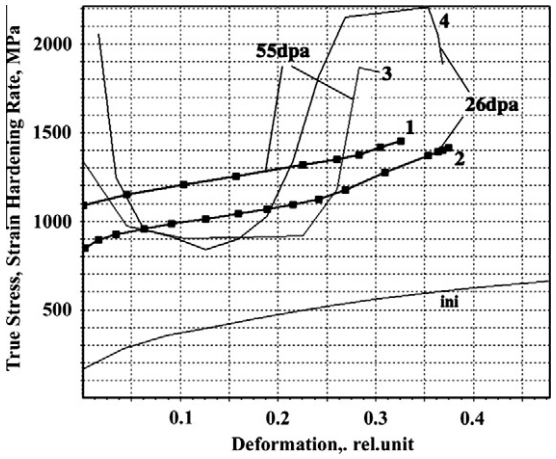

Fig. 5. Curves of "σ–ε" (#1, 2, ini) and "$d\sigma/d\varepsilon$–ε" (3, 4) for unirradiated 12Cr8Ni10Ti specimen (ini), 26 dpa (#2, 4) and 55 dpa (#1, 3) specimens. Specimens were tested at 20 °C. The dimensions and scale for the $d\sigma/d\varepsilon$–ε curves are the same as for the "σ–ε" curves.

yield point, the derivative $d\sigma/d\varepsilon$–ε reduces to negative values, and the neck begins to develop. Thereafter a smooth upward trend is observed in the "σ–ε" curve. As $d\sigma/d\varepsilon$ increases the value of "$d\sigma/d\varepsilon$–ε" becomes positive, indicating that the strain hardening rate is increasing strongly. When ~30–35% martensite has formed, no further local hardening occurs as the deformation and the nascent neck shifts to neighboring, less deformed material.

In a study by Lapin and coworkers this same steel was tested at 20 °C after irradiation at 100–300 °C in the RFT reactor [12]. They observed a tendency for elongation to exhibit a minimum at relatively low dpa levels and then tend to increase at higher dose. There were no observations made by Lapin of the mode of elongation or the details of the specimen post-tensile morphology, however. In another study by Pecherin and coworkers [13] two steels with a greater propensity toward martensite instability (08Cr18Ni9 and 03Cr16Ni9Mo2) were irradiated in the BOR-60 reactor to doses ~3 dpa at 300–320 °C. These were found to develop increased engineering ductility at room temperature and below compared to behavior observed at either lower dose or higher test temperature. X-ray studies confirmed the formation of radiation–acceleration of deformation martensite but the moving wave phenomenon, if present, was not observed.

It has been shown that low temperature deformation of highly voided stainless steel can involve martensite instability leading to failure [14]. Based on these results it appears that irradiation at relatively low temperatures increases the instability of steels 12Cr18Ni10Ti and 08Cr16Ni11Mo3 to martensitic transformation in the absence of significant void swelling. Studies of Kadyrzhanov and Maksimkin have shown radiation-enhanced formation of deformation-induced martensite indeed occurs under a variety of radiation conditions, especially at lower irradiation temperatures [15]. This radiation-induced propensity toward instability follows the known behavior of martensite transformation, increasing at lower levels of nickel and also at lower deformation temperatures. It is not yet clear why this propensity develops at higher doses and whether it might be related to some long-term consequence of transmutation and/or segregation.

5. Conclusions

Deformation waves have been observed at relatively low deformation temperatures in low-nickel steels irradiated in the BN-350 fast reactor to doses above ~20 dpa. As the nickel level or the deformation temperature increases it is harder to initiate these waves. This mechanism involves a moving wave of plastic deformation that precludes necking and thereby produces anomalously high values of engineering ductility, especially when compared to deformation occurring at lower neutron exposures. The mechanism has been shown to arise from martensite instability enhanced by irradiation, leading to a strong increase in the strain hardening rate.

Acknowledgements

The Kazakh portion of this work was supported by the Ministry of Energy and Mineral Resources of the Republic of Kazakhstan. The early part of the US portion was sponsored by the Office of Fusion Energy Sciences, US Department of Energy under Contract DE-AC06-76RLO at Pacific Northwest National Laboratory and the final part was completed by F.A. Garner of Radiation Effects Consulting.

References

[1] M.N. Gusev, O.P. Maksimkin, I.S. Osipov, F.A. Garner, J. Nucl. Mater. 386–388 (2009) 273–276.
[2] O.P. Maksimkin, M.N. Gusev, I.S. Osipov, Inf. News Natl. Nucl. Center Republic Kazakhstan 1 (2005) 46.
[3] M.N. Gusev, O.P. Maksimkin, I.S. Osipov, F.A. Garner, Application of digital marker extensometry to determine the true stress–strain behavior of irradiated metals and alloys, in: Proc. of 5th Int. Symposium on Small

Specimen Test Technology, ASTM STP 1502, 2009, pp. 79–92 (on-line at ASTM as paper ID JAI101001).
[4] J. Talonen, P. Aspegren, H. Hanninen, Mater. Sci. Technol. (2004) 1506.
[5] S.K. Fawad, Quantitative Analysis of Multi-phase Systems – Steels with Mixture of Ferrite and Austenite. PhD Thesis, Institute of Technology, Department of Physics and Measurement Technology, Linköping University, Sweden, 2005.
[6] O.P. Maksimkin, M. N Gusev, I.S. Osipov, Bull. Natl. Nucl. Center 3 (3) (2007) 3–17 (in Russian).
[7] E. Nagy, V. Mertinger, F. Tranta, J. Sólyom, Mater. Sci. Eng., A 378 (2004) 308.
[8] G. Was, Fundamentals of Radiation Materials Science, Springer, 2007.
[9] V.N. Voyevodin, I.M. Neklyudov, Evolution of the Structure Phase State and Radiation Resistance of Structural Materials, Kiev, Naukova Dumka, 2006 (in Russian).
[10] F. A. Garner, Irradiation performance of cladding and structural steels in liquid metal reactors, in: Materials Science and Technology: A Comprehensive Treatment, Vol. 10A, VCH Publishers, 1994, p. 419 (Chapter 6).
[11] A.M. Parshin, Structure Resistibility and Radiation Damage in Corrosion-resistant Steels and Alloys, Chelyabinsk Department, Chelyabinsk, Metallurgy, 1988, p. 656 (in Russian).
[12] A.N. Lapin, V.A. Nikolaev, I.A. Razov, Fiz. Khim. Obrab. Mater. 1 (1970) 9 (in Russian).
[13] A.M. Pecherin, V.K. Shamardin, Yu.D. Goncharenko, V.A. Krasnoselov, VANT – Quest. Atom. Sci. Tech. #5 (47) (1988) 1–65.
[14] M.L. Hamilton, F.H. Huang, W.J.S. Yang, F.A. Garner, Mechanical properties and fracture behavior of 20% cold-worked 316 stainless steel irradiated to very high exposures, in: F.A. Garner, N. Igata, C.H. Henager, Jr. (Eds.), Effects of Radiation on Materials: Thirteenth International Symposium (Part II) Influence of Radiation on Material Properties, ASTM STP 956, ASTM, Philadelphia, PA, 1987, p. 245.
[15] K.K. Kadyrzhanov, O.P. Maksimkin, Martensitic transformations in neutron irradiated and helium implanted stainless steels, in: 21st International Symposium on Effects of Radiation on Materials, ASTM STP, vol. 1447, 2004, pp. 105–116.